HHS Public Access

Author manuscript

J Proteome Res. Author manuscript; available in PMC 2017 February 05.

Published in final edited form as:

J Proteome Res. 2016 February 5; 15(2): 563–571. doi:10.1021/acs.jproteome.5b00957.

The Anti-Oxidant Drug Tempol Promotes Functional Metabolic Changes in the Gut Microbiota

Jingwei Cai[†], **Limin Zhang**[†,‡], **Richard A. Jones**[†], **Jared B. Correll**[†], **Emmanuel Hatzakis**[||], **Philip B. Smith**[§], **Frank J. Gonzalez**[¶], and **Andrew D. Patterson**[†,*]

[†]Center for Molecular Toxicology and Carcinogenesis, Department of Veterinary and Biomedical Sciences, Pennsylvania State University, University Park, State College, Pennsylvania, 16802, USA

[‡]CAS Key Laboratory of Magnetic Resonance in Biological Systems, State Key Laboratory of Magnetic Resonance and Atomic and Molecular Physics, National Centre for Magnetic Resonance in Wuhan, Wuhan Institute of Physics and Mathematics, Chinese Academy of Sciences (CAS), Wuhan 430071, China

[§]Metabolomics Facility, Huck Institutes of Life Sciences, Pennsylvania State University, University Park, State College, Pennsylvania, 16802, USA

[||]Department of Chemistry, Pennsylvania State University, University Park, Pennsylvania, 16802, USA

[¶]Laboratory of Metabolism, National Cancer Institute, NIH, Bethesda, Maryland, 20892, USA

Abstract

Recent studies have identified the important role of the gut microbiota in the pathogenesis and progression of obesity and related metabolic disorders. The antioxidant tempol was shown to prevent or reduce weight gain and modulate the gut microbiota community in mice; however, the mechanism by which tempol modulates weight gain/loss with respect to the host and gut microbiota has not been clearly established. Here we show that tempol (0, 1, 10, and 50 mg/kg p.o. for 5 days) decreased cecal bacterial fermentation and increased fecal energy excretion in a dose-dependent manner. Liver ^{1}H NMR-based metabolomics identified a dose-dependent decrease in glycogen and glucose, enhanced glucogenic and ketogenic activity (tyrosine and phenylalanine), and increased activation of the glycolysis pathway. Serum ^{1}H NMR-based metabolomics indicated that tempol promotes enhanced glucose catabolism. Hepatic gene expression was significantly altered as demonstrated by an increase in *Pepck and G6pase* and a decrease in *Hnf4a*, *ChREBP*, *Fabp1*, and *Cd36* mRNAs. No significant change in the liver and serum metabolomic profiles were

[*]To whom correspondence should be addressed. adp117@psu.edu; Tel: 814-867-4565.

SUPPORTING INFORMATION

Two dimensional ^{1}H-^{1}H total correlation spectroscopy (TOCSY) NMR for SCFAs identification (Figure S1); Body weight and liver to body to weight ratio change; liver histology (Figure S2); GC-MS Quantification of cecal SCFAs and BCAAs in mice gavaged with 100 mg/kg tempol for 5 days (Figure S3A–B); O-PLS-DA scores and correlation coefficient-coded loadings plots for ^{1}H NMR based cecal metabolites analysis of mice treated with 100 mg/kg tempol for 5 days (Figure S3C); O-PLS-DA scores and correlation coefficient-coded loadings plots for the models from NMR spectra of cecal content and feces obtained from different dose of tempol-treated mice (Figure S4); quantification of gross heat of feces by bomb calorimetry (Figure S5); quantitative PCR analysis of universal 16s rRNA gene of fecal microbiome (Figure S6); primer sequences for qPCR analysis of genes associated with glucose and lipid metabolic pathway (Table S1); bacterial primer sequences (Table S2).

observed in germ-free mice thus establishing a significant role for the gut microbiota in mediating the beneficial metabolic effects of tempol. These results demonstrate that tempol modulates the gut microbial community and its function resulting in reduced host energy availability and a significant shift in liver metabolism towards a more catabolic state.

Keywords

SCFAs; metabolomics; GC-MS; NMR; bomb calorimetry; tempol; obesity

INTRODUCTION

Obesity and related metabolic disorders are major public health concerns. Previous studies identified the gut microbiota as an important factor involved in metabolic homeostasis due to their role in extracting energy from the diet[1], interfering with metabolic signaling[2], and modulating gut inflammation[3]. The population and functions of the gut microbiota can be manipulated by xenobiotics (e.g., antibiotics)[4, 5], pathogens (e.g., diarrhea-causing organisms)[6], drugs[7], and host genetic factors[8]. Additionally, the gut microbiota has been identified as a promising target for therapeutic intervention to treat metabolic disorders including obesity[9].

Tempol (4-hydroxy-2,2,6,6-tetramethylpiperidine-N-oxyl) is a water soluble nitroxide, stable free radical, which has been reported to be an effective antioxidant in detoxifying reactive oxygen species in cell culture and animal studies[10, 11]. Tempol was reported to inhibit body weight gain in mice[12] and can dramatically influence non-alcoholic fatty liver disease (NAFLD) through alterations in signaling between the gut microbiota and the farnesoid X receptor (FXR)[13]. The protective effects of tempol against NAFLD were found to be mediated specifically through changes in the composition of the gut microbiota, attenuated FXR signaling, and inhibition of hepatic SREBP1C and de novo lipogenesis[14]. Based on these previous studies, the anti-obesity effect of tempol is strongly associated with alterations in the gut microbiota and host signaling axis.

The gut microbiota has been implicated in host metabolic status mainly through its control of energy availability by fermenting non-digestible dietary fiber into available, absorbable, and transportable short chain fatty acids (SCFAs). SCFAs are saturated fatty acids with aliphatic tails with less than six carbons, among which acetate (C2), propionate (C3), butyrate (C4) are most abundant[15]. Acetate is the most abundant SCFAs in the gut compared to propionate and butyrate[16]. SCFAs of bacterial metabolic activity account for about 5–10% of daily energy intake of the host[17]. Overall the host reabsorbs and utilizes SCFAs as an energy source or as anabolic substrates for processes including de novo lipogenesis[18].

In the current study, modulation of host energy metabolism by tempol through changes in gut microbiota fermentation was explored. Cecal contents and fecal SCFA concentrations, fecal energy excretion, liver and serum metabolite profiles investigated via combined ^{1}H NMR-based metabolomics and targeted GC-MS profiling, bomb calorimetry, and hepatic gene expression were used to assess changes in mice after 5 day intragastric administration of tempol. Notably, a dose-dependent decrease in bacterial fermentation was found in

tempol-treated mice along with significant changes in liver metabolism. Metabolic changes were found to be microbial dependent. This study provides an additional mechanism for the anti-obesity effect of tempol mediated by the gut microbiota.

MATERIALS AND METHODS

Chemicals

Tempol, short chain fatty acids, 1-propanol, propyl chloroformate, pyridine, sodium chloride, K_2HPO_4, and NaH_2PO_4 were purchased from Sigma-Aldrich Chemical Co. Ltd. (St. Louis, MO). Hexane and methanol were purchased from EMD Chemicals Inc (Gibbstown, NJ). The internal standard hexanoic acid-6,6,6-d_3 was obtained from C/D/N Isotopes Inc (Pointe-Claire, Quebec, Canada). Sodium 3-trimethylsilyl [2,2,3,3-d_4] propionate (TSP-d_4) and D_2O (99.9% in D) were purchased from Cambridge Isotope Laboratories (Miami, FL). Standard benzoic acid pellets were purchased from Parr Instrument Company (Moline, IL). All compounds were of the highest analytical grade available.

Tempol Treatment and Sample Collection

C57BL/6J wild-type male mice (4-week-old) were purchased from the Jackson Laboratory (Bar Harbor, Maine). The mice were housed in polypropylene cages with corncob bedding in a controlled environment (temperature, 65–75°F; relative humidity, 30%–70%; photoperiod, 12 h light/dark cycle). Water and regular chow were supplied ad libitum. Mice were randomly grouped after one-week acclimatization before treatment. Tempol (dissolved in 0.9% saline) was administered in the morning by gavage for 5 consecutive days. The control group was administered an equivalent volume of 0.9% saline. Mice were transferred to nalgene metabolic cage systems (Tecniplast, USA) and housed individually for 24 hours during the acclimatization period and treatment period every other day for fecal sample collection. Mice were weighed in the mornings and killed on day 6. Liver, cecal contents, and serum samples were collected immediately following CO_2 asphyxiation. All samples were quickly placed in liquid nitrogen then stored at −80 °C for future analysis. All procedures were performed in accordance with the Institute of Laboratory Animal Resources guidelines and approved by the Pennsylvania State University Institutional Animal Care and Use Committee. Germ-free mice wild-type C57Bl/6J mice were bred and maintained by the Pennsylvania State University Gnotobiotic Facility, housed in germ-free isolators, and fed an autoclaved diet. All materials and supplies were sterilized before transfer into the isolators. Germ-free status was monitored continuously and confirmed through a series of culture based assays.

Gas Chromatography–Mass Spectrometry (GC-MS) Analysis

SCFAs level in tissues were measured with a targeted protocol as described previously[19]. 50 mg of cecal content or feces were mixed with 1 mL of 0.005 M aqueous NaOH containing internal standard hexanoic acid-6,6,6-d_3 (5 μg/mL), homogenized (Bertin Technologies, Rockville, MD) at 6500 rpm,1 cycle, 60s and then centrifuged (Eppendorf, Hamburg, Germany) at 13,200 × g at 4 °C for 15 min. The supernatant was collected and an aliquot of 500 μL of a solvent mixture of 1-propanol/pyridine (3/2, v/v) and 100 μL of propyl

chloroformate was subsequently added to the supernatant and briefly vortexed. Samples were heated (Thermo Scientific, Marietta, OH) at 60 °C for 1 hour. The derivatized samples were extracted with a two-step hexane extraction. 300 μL of hexane was added to the sample, vortexed for 30 s, and then centrifuged (2000 × g, 4 °C for 5 min). 300 μL of the upper layer was transferred to a glass auto sampler vial for GC-MS analysis. Another 200 μL of hexane was added to the sample and the extraction repeated and combined with the previous upper layer. Samples were analyzed using a 7890A gas chromatograph coupled with an Agilent 5975C mass selective detector (Agilent Technologies, Santa Clara, CA). A HP-5-MS (5 %-diphenyl 95%-methylpolysiloxane) capillary GC column (30 m × 250 μm i.d. 2.5μm film thickness, Agilent Technologies) was used with helium as the carrier gas at a constant flow rate of 1 mL/min. 0.5 μL sample was injected onto the column using a pressure pulsed split (10 psi, split ratio 10/1) The initial column temperature was set at 55 °C for 0.5 min and then increased to 70 °C at a rate of 10 °C/min, increased to 85 °C at a rate of 3 °C/min, increased to 110 °C at a rate of 5 °C/min, increased to a final temperature of 290 °C at a rate of 30 °C/min which was held for 5 minutes. The temperatures of the front inlet, transfer line and mass source were set at 260 °C, 290 °C, 230 °C. Mass spectral data was collected in a full scan mode over the a mass range 35–500 *m/z* with an electron energy of 70eV. All raw data were processed with Enhanced Chemstation (Agilent Technologies) for mass spectral visualization, identification, and quantitation. The integrated areas of the SCFAs were normalized to the internal standard and quantified with a standard curve constructed from serial dilutions (2500 μM, 1250 μM, 625 μM, 315 μM, 156.25 μM, 78.125 μM, 0) of SCFAs.

Nuclear Magnetic Resonance (NMR) Spectroscopy Sample Preparation

Cecal content or fecal samples (50 mg-100 mg) were mixed with 800 μL of phosphate buffer (K_2HPO4/NaH_2PO4, 0.1 M, pH 7.4, 50% v/v D_2O) containing 0.005% TSP-d4 as a chemical shift reference (δ 0.00 ppm). The sample was freeze/thawed three times with liquid nitrogen then homogenized (Precellys 24, Bertin Technologies, Rockville, MD) and centrifuged (13,200 × g, 4 °C) for 10 min. The supernatant was transferred to a new microcentrifuge tube and another 400 μL of PBS was added to the pellets and the above procedure repeated. The supernatants were combined, centrifuged (13,200 × g, 4 °C, 10 min), and 550 μL was transferred to NMR tubes. Liver tissues (50 mg) were extracted three times with 600 μL of precooled methanol-water mixture (2/1, v/v) using the Precellys tissue homogenizer. After homogenization and centrifugation (13,200 × g, 4°C, 10 min), the combined supernatants were dried and reconstituted in 600 μL phosphate buffer (K2HPO4/ NaH2PO4, 0.1M, pH 7.4, containing 50% D_2O and 0.005% TSP-d_4). After centrifugation (13,200 × g, 4 °C, 10 min), 550 μL of each extract was transferred into an NMR tube for analysis. Serum samples (200 μL) were combined with 400 μL of phosphate buffer (K_2HPO4/NaH_2PO4, 45mM, pH 7.4, 50% v/v D_2O containing 0.9% NaCl) and centrifuged (13,200 × g, 4 °C, 10 min). 550 μL of supernatant was transferred into NMR tubes for analysis.

^{1}H NMR Spectroscopy, Spectral Data Processing, and Multivariate Data Analysis

^{1}H NMR-based metabolomic analysis was performed as previously described[20]. Color-coded loading plots were generated from the O-PLS-DA models using a script for MATLAB

(The Mathworks Inc.; Natick, MA). O-PLS-DA scores represent the model power and the color-coded correlation coefficient indicates the significance of the metabolite contribution to the class separation, with a “hot” color (e.g., red) being more significant than a “cold” color (e.g., blue). In this study, a cutoff value of $|r| > 0.707$ ($r > 0.707$ and $r < -0.707$) was chosen for correlation coefficient as significant based on the discrimination significance ($p \leq 0.05$). SCFAs in cecal content and feces were assigned with two dimensional ^{1}H-^{1}H total correlation spectroscopy (TOCSY) NMR (Figure S1). Relative content of each SCFA is determined by NMR peak area of SCFA relative to internal standard (TSP-d_4).

Bomb Calorimetry

Bomb calorimetry was performed using a 6200 isoperibol calorimeter (Parr Instrument Company, Moline, IL). Dried fecal samples (100 mg) were weighed and ground in a clean mortar and pestle. Ground samples were pressed into ¼ inch diameter pellets (Parr 2812 Pellet Press, Moline, IL). The remaining moisture content was removed from the fecal pellet using a speedvac concentrator (Thermo Fisher Scientific, Marietta, OH). Benzoic acid pellets were used for standardization and optimization of the bomb calorimeter. Samples were placed in a tared fuel capsule (208AC) in the 1109A semi-micro oxygen bombs (Parr Instrument Company, Moline, IL) and fixed by a coiled 10 cm of NiCr fuse wire (PN 45C10). A minimum 99.5% purity oxygen was provided with 420 psi pressure to the bomb. Prepared semi-micro bomb were set on a ring support in the A604DD twin-chambered calorimeter bucket. Gross heat of samples were determined by the temperature change recorded during combustion and expressed as calories/gram feces.

Quantitative PCR analysis

Liver (50 mg) was extracted using TRIzol reagent (Invitrogen, Carlsbad, CA). DNA concentration was determined by Nanodrop. cDNA was synthesized from 1 μg of total RNA using qScript cDNA SuperMix (Quanta Biosciences, Gaithersburg, MD) and then were diluted to 1μg/μL before subjected to quantitative PCR. QPCR was performed using SYBR green QPCR master mix on an ABI Prism 7900HT Fast Real-Time PCR sequence detection system (Applied Biosystems, Foster City, CA). QPCR conditions were 95°C for 20 s; 95 °C for 0.01 s; 60 °C for 20 s; 95 °C for 15 s; 60 °C for 15 s and 95 °C for 15 s, 40 cycles. The reactions were analyzed according to the ΔΔCT method. All targeted mRNA were normalized to the GADPH mRNA as an internal control.

Data Analysis

Graphical illustrations and statistical analysis were performed using Prism GraphPad version 6. All data values were expressed as mean ± SEM. $p<0.05$ was considered significant.

RESULTS

Tempol influences weight gain and preserves liver function in a dose-dependent manner

To determine if the observed anti-obesity effect of tempol is dose-dependent, mice were treated with tempol (0, 1, 10, 50 mg/kg) by gavage for 5 consecutive days. The control group and 1 mg/kg tempol group mice showed a 1.5% increase in body weight per day over the treatment period (Figure S2A). However, the body weight gain for 10 mg/kg tempol treated

mice showed a similar rate (1.5% per day) for the first two days, and then decreased to 0.47% per day from day 2 to day 5. The 50 mg/kg tempol-treated mice showed significant weight loss over the entire study (1.65% per day). This data demonstrates that the body weight gain is inversely associated with the tempol dose. Change in body weights were not due to toxicity, as no change in wet liver weight to body weight ratio was observed (Figure S2B). Additionally, liver histology (Figure S2C) showed no morphological difference between control and tempol treated groups, further indicating that tempol treatment did not cause substantial physiological and histological abnormalities.

Tempol modulates SCFAs availability in gut

It was reported that fecal SCFA concentrations are significantly higher in obese than lean counterparts[21, 22]. In agreement with this finding, decreased cecal SCFAs were found in 100 mg/kg, tempol-treated mice (Figure S3), suggesting that tempol inhibits bacterial fermentation and decreases SCFAs availability in the lower gut. To determine whether the SCFAs inhibition effect of tempol is dose-dependent, SCFA levels were measured in mice treated with different doses of tempol by global ^{1}H NMR metabolomics and targeted GC-MS analysis. As shown in Figure 1A–D, a dose-dependent decrease of SCFAs was observed in extracts from the cecal content and feces upon tempol with the most significant decrease observed in the 50 mg/kg dose group. Specifically, when compared with control, the 50 mg/kg group exhibited a 41%, 25% and 39% decrease in cecal acetate, propionate, and butyrate, respectively, as identified by ^{1}H NMR. These changes were confirmed by GC-MS revealing a 28%, 63% and 37% decrease in cecal acetate, propionate and butyrate, respectively. In feces, a 50%, 36%, 21% decrease of acetate, propionate and butyrate and a 42%, 41%, 33% decrease of acetate, propionate and butyrate were identified by ^{1}H NMR and GC-MS, respectively. In general, higher amount of SCFAs were measured in the cecal contents than from feces by GC-MS quantification, indicating the SCFAs reabsorption and utilization occurred as the cecal contents passed through the colon. Interestingly, in the 50 mg/kg tempol group, an increase of amino acids (tyrosine and phenylalanine), nitrogenous bases (uracil) and the nitrogenous base derivative (hypoxanthine) were identified as being significantly changed in the cecum (Figure S4A) suggesting further alterations in amino acid and nucleotide metabolism in the small intestine.

Tempol-treated mice excrete more energy

Analysis of fecal metabolites revealed a dose-dependent increase of glucose and oligosaccharides in tempol-treated groups (Figure 1C), which are substrates for microbial fermentation. This observation suggests decreased microbial fermentation ability of tempol-treated mice. To further validate these findings, bomb calorimetry was performed to determine the energy loss into feces (Figure S5). The feces collected from metabolic cages after the final dosing with tempol was used for gross heat measurements. The results demonstrated that as the tempol dose increased, there was a proportional increase in the total gross heat measured in the fecal pellets. Specifically, one gram of feces from the 50 mg/kg tempol treated mice contains, on average, 139 more calories compared to control mice. The increased fecal energy excretion is consistent with the decreased energy availability revealed by lower SCFA production after tempol treatment.

Tempol-mediated metabolic changes in liver are microbiota dependent

To further determine the impact of tempol on energy metabolism, the liver metabolome was measured by ^{1}H NMR. No hepatic metabolite differences were identified for the 1 mg/kg dose (Figure 2A). However, at the 50 mg/kg dose, reduced glycogen, sugars, and amino acids were identified and indicative of increased hepatic energy storage mobilization. The glucogenic and ketogenic amino acids phenylalanine and tyrosine, which promote catabolism for energy availability[23] were increased. Additionally, uridine, a nucleoside involved in glycolysis was upregulated in the 50 mg/kg tempol group compared to control. Another immunoprotective and neuroprotective nucleoside, inosine[24], was upregulated. These results suggest that the overall liver metabolism balance shifted from energy storage to energy generation.

Although observations in the current and previous studies suggested that tempol changes the gut microbiota and causes metabolic alterations in the liver, it is unclear whether these changes are a direct effect of tempol administration or are microbiota-mediated. The germ-free mouse liver metabolome was unchanged by 50 mg/kg tempol treatment as observed in conventionally-raised mice (Figure 2B), indicating the microbiota play a vital role in directing metabolic alterations with tempol.

Tempol-altered microbiota result in altered serum metabolites

Similar to the ^{1}H NMR metabolomic profiles of the liver, a significant dose-dependent effect was identified in the serum of conventionally-raised mice (Figure 3A). No significant changes were seen in the 1 mg/kg tempol treated mice, while a variety of metabolites were altered in the 10 mg/kg and 50 mg/kg groups. Specifically, pyruvate, lactate, and citrate were increased while glucose was markedly decreased, indicating upregulation of glycolysis. However, the germ-free mouse serum profile was not significantly changed compared to control (Figure 3B), again demonstrating that the induced metabolic shifts by tempol are microbiota-dependent.

Tempol alters hepatic gene expression involved in glucose and lipid metabolism

To further investigate the molecular mechanisms associated with the observed metabolic changes, the expression of genes associated with glucose and lipid metabolic pathway were analyzed by QPCR. The 50 mg/kg tempol treatment group had significantly increased hepatic expression of *Pepck and G6pase* mRNA by one to two fold in conventionally-raised mice (Figure 4A), indicating upregulation of gluconeogenesis and glycolysis. Moreover, an overall decrease or decreased trend of hepatic expression of *Hnf4a*, *ChREBP*, *Fabp1*, *Fabp2, Fabp5*, and *Cd36* mRNAs encoding adipogenic transcription factors and proteins were detected in the conventional 50 mg/kg tempol treated mice (Figure 4B). These results suggest down regulation of de novo lipogenesis and improvement of lipid metabolism, consistent with the obesity-resistant phenotype observed with tempol. No significant changes in the expression of these genes were identified in germ-free tempol-treated mice, again demonstrating the effects of tempol are highly dependent on the gut microbiota.

DISCUSSION

Here we proposed that tempol restricts energy availability in the host through inhibition of microbial SCFA production. Other studies reported greater colonic SCFA production in overweight and obese individuals compared to lean counterparts in humans independent of dietary intake[21–22, 25]. These observations indicate SCFA metabolism plays a significant role in obesity. Consistently, the anti-obesity compound tempol decreases cecal and fecal acetate, propionate, and butyrate levels in a dose-dependent manner. Moreover, the substrates for microbial fermentation, glucose and oligosaccharides, were excreted in greater quantities into feces in tempol treated mice. Thus it is likely that the reduced energy-harvesting potential of tempol-altered gut microbiota contributes to the metabolic improvements observed in models of diet-induced obesity[2, 26].

In addition to the restriction in energy availability, tempol profoundly impacts the overall metabolism of the host. SCFAs are not only direct energy substrates for tissues but also substrates for gluconeogenesis (e.g., propionate)[27–28] and lipogenesis[18]. For gluconeogenesis, propionate acts as a precursor[29–30] which is first converted to propionyl-CoA and then to succinyl-CoA. Succinyl-CoA enters the citrate cycle to generate oxaloacetate, the direct precursor for gluconeogenesis. Therefore, restricted SCFAs availability would be expected to lead to downregulated glucose levels and decreased products like glycogen and glucose. As expected, with tempol treatment, an overall decrease in glycogen, sugars, and amino acid reserves were observed in liver, suggesting decreased glucose anabolism and increased glucose catabolism, consistent with a lean phenotype and the previously described insulin sensitivity improvement effect of tempol[31]. Moreover, elevated hepatic acetate levels suggest increased fatty acid catabolism, as acetate is an end product of fatty acid oxidation in liver peroxisomes[32, 33]. The glucogenic and ketogenic essential amino acids phenylalanine and tyrosine are important for energy generation and they are also precursors of thyroid hormone and catecholamines (e.g., dopamine, epinephrine, norepinephrine) that act on adipose tissue to modulate lipolysis and thermogenesis[23]. An upregulation of phenylalanine and tyrosine in the liver of tempol treated mice might indicate an alteration in energy production and lipid metabolism. Previous mouse studies suggested the serum glucose levels were decreased through caloric restriction[34, 35]. Further, serum glucose levels are positively correlated with body mass index (BMI) observed in human studies[36, 37]. Tempol serum metabolite profiles identified decreased glucose and amino acids levels consistent with the decreased hepatic glucose and amino acid reserves, improved insulin sensitivity, and lean phenotype. Lactate is derived from anaerobic glycolysis and subcutaneous fat[38, 39], which is also a major precursor for gluconeogenesis. Elevated lactate in liver and serum is consistent with upregulated glucose utilization and fat mobilization.

Alterations in the expression of key hepatic genes associated with glucose and lipid metabolic pathways further confirmed the metabolic changes revealed by metabolomic analysis. PEPCK is a rate-controlling enzyme in gluconeogenesis and its mRNA was upregulated in the 50 mg/kg tempol treated livers of conventional mice. mRNA encoding *G6Pase*, the key enzyme in gluconeogenesis and glycogenolysis that hydrolyzes glucose-6-phosphate to free glucose that can then enter circulation[40], was increased in the 50 mg/kg

tempol group. Glycogenolysis and gluconeogenesis are two pathways to generate glucose from either glycogen or non-carbohydrate precursors. Both pathways are upregulated in tempol-treated group likely due to an adaptive response of liver in attempt to restore glucose levels. As glucose utilization is accelerated with tempol treatment, hepatic glucose levels are reduced. In order to keep up with the demand for glucose utilization, the liver compensates by mobilizing glucogenic pathways. Primarily, glycogenolysis is upregulated to free glucose from glycogen. Secondarily, gluconeogenesis is activated to generate more glucose from non-carbohydrate substrates. The upregulated glycogenolysis and gluconeogenesis pathways along with the upregulated hepatic gene expression with tempol treatment are consistent with the decreased hepatic glucose reserves and increased hepatic gluconeogenic precursors (phenylalanine and tyrosine) revealed by ^{1}H NMR-based liver metabolomic profiling. There was an increasing trend of *Glut2* mRNA as well, typically increased with improved insulin sensitivity as seen in type II diabetes[41]. Besides glucose metabolism related genes, mRNAs encoding transcription factors *Hnf4a and ChREBP*, and lipogenic proteins *Fabp1 and Cd36* were downregulated. The downregulation of genes involved in lipid metabolism in conventional tempol treated mice reveals inhibition of *de novo* lipogenesis by tempol which also explains the observed adiposity-resistant phenotype of conventional tempol treated mice.

Metabolomic profiling of conventional tempol-treated mice suggests an energy balance shift from storage to substrate breakdown and energy generation to compensate for the reduced production of SCFAs. For example, we observed an increase in the glycogenolysis, glycolysis, and lipolysis pathways. It is likely that the combined effects of these pathways all contribute to the observed anti-obesity phenotyped in tempol-treated mice. Furthermore, these effects were highly dependent on the gut microbiota as germ-free mice treated with tempol had no significant changes in their serum or liver metabolomic profiles.

Obese microbiota community structure analysis from mouse and human studies were characterized by an elevated Firmicutes to Bacteriodetes ratio[26, 42–44] indicative of better fermentation capacity with greater energy harvesting potential from the microbial community. Consistent with previous studies[13], a decreased Firmicutes to Bacteriodetes ratio was observed in the 50 mg/kg tempol group on a normal chow diet (Figure S6B). Other microbial changes reported with tempol treatment including decreasing abundance of β-Proteobacteria and *Lactobacillus* spp., were also confirmed in this study (Figure S6C–D). Overall, tempol helps promote a more obesity resistant gut microbial community which provides a better environment for energy restriction and metabolic regulation.

The anti-obesity effects of tempol have been associated with its anti-oxidative stress properties[31, 45]. Here, by comparing conventionally-raised and germ-free mice, the current studies demonstrated that tempol exerts its anti-obesity effect, in part, through interactions with the gut microbiota and the host. Further, the tempol-altered microbiota is sufficient to promote the obesity resistant phenotype by causing metabolic changes from energy storage to expenditure.

Supplementary Material

Refer to Web version on PubMed Central for supplementary material.

Acknowledgments

This work was supported by National Institute of Environmental Health Sciences [ES022186 (ADP)].

References

1. Wichmann A, Allahyar A, Greiner TU, Plovier H, Lunden GO, Larsson T, Drucker DJ, Delzenne NM, Cani PD, Backhed F. Microbial modulation of energy availability in the colon regulates intestinal transit. Cell Host Microbe. 2013; 14(5):582–90. [PubMed: 24237703]
2. Turnbaugh PJ, Ley RE, Mahowald MA, Magrini V, Mardis ER, Gordon JI. An obesity-associated gut microbiome with increased capacity for energy harvest. Nature. 2006; 444(7122):1027–31. [PubMed: 17183312]
3. Guarner F, Malagelada JR. Gut flora in health and disease. Lancet. 2003; 361(9356):512–9. [PubMed: 12583961]
4. Jernberg C, Lofmark S, Edlund C, Jansson JK. Long-term ecological impacts of antibiotic administration on the human intestinal microbiota. ISME J. 2007; 1(1):56–66. [PubMed: 18043614]
5. Jakobsson HE, Jernberg C, Andersson AF, Sjolund-Karlsson M, Jansson JK, Engstrand L. Short-term antibiotic treatment has differing long-term impacts on the human throat and gut microbiome. PloS one. 2010; 5(3):e9836. [PubMed: 20352091]
6. Pop M, Walker AW, Paulson J, Lindsay B, Antonio M, Hossain MA, Oundo J, Tamboura B, Mai V, Astrovskaya I, Corrada Bravo H, Rance R, Stares M, Levine MM, Panchalingam S, Kotloff K, Ikumapayi UN, Ebruke C, Adeyemi M, Ahmed D, Ahmed F, Alam MT, Amin R, Siddiqui S, Ochieng JB, Ouma E, Juma J, Mailu E, Omore R, Morris JG, Breiman RF, Saha D, Parkhill J, Nataro JP, Stine OC. Diarrhea in young children from low-income countries leads to large-scale alterations in intestinal microbiota composition. Genome Biol. 2014; 15(6):R76. [PubMed: 24995464]
7. Touw K, Wang YW, Leone V, Nadimpalli A, Nathaniel H, Gianricol F, Kashyap P, Chang E. Drug-induced constipation alters gut microbiota stability leading to physiological changes in the host. FASEB J. 2014; 28(1)
8. Benson AK, Kelly SA, Legge R, Ma F, Low SJ, Kim J, Zhang M, Oh PL, Nehrenberg D, Hua K, Kachman SD, Moriyama EN, Walter J, Peterson DA, Pomp D. Individuality in gut microbiota composition is a complex polygenic trait shaped by multiple environmental and host genetic factors. Proc Natl Acad Sci U S A. 2010; 107(44):18933–8. [PubMed: 20937875]
9. Jia W, Li H, Zhao L, Nicholson JK. Gut microbiota: a potential new territory for drug targeting. Nat Rev Drug Discov. 2008; 7(2):123–9. [PubMed: 18239669]
10. Wilcox CS. Effects of tempol and redox-cycling nitroxides in models of oxidative stress. Pharmacol Ther. 2010; 126(2):119–45. [PubMed: 20153367]
11. Francischetti IM, Gordon E, Bizzarro B, Gera N, Andrade BB, Oliveira F, Ma D, Assumpcao TC, Ribeiro JM, Pena M, Qi CF, Diouf A, Moretz SE, Long CA, Ackerman HC, Pierce SK, Sa-Nunes A, Waisberg M. Tempol, an intracellular antioxidant, inhibits tissue factor expression, attenuates dendritic cell function, and is partially protective in a murine model of cerebral malaria. PloS one. 2014; 9(2):e87140. [PubMed: 24586264]
12. Kim CH, Mitchell JB, Bursill CA, Sowers AL, Thetford A, Cook JA, van Reyk DM, Davies MJ. The nitroxide radical TEMPOL prevents obesity, hyperlipidaemia, elevation of inflammatory cytokines, and modulates atherosclerotic plaque composition in apoE−/− mice. Atherosclerosis. 2015; 240(1):234–41. [PubMed: 25818249]
13. Li F, Jiang C, Krausz KW, Li Y, Albert I, Hao H, Fabre KM, Mitchell JB, Patterson AD, Gonzalez FJ. Microbiome remodelling leads to inhibition of intestinal farnesoid X receptor signalling and decreased obesity. Nat Commun. 2013; 4:2384. [PubMed: 24064762]

14. Jiang C, Xie C, Li F, Zhang L, Nichols RG, Krausz KW, Cai J, Qi Y, Fang ZZ, Takahashi S, Tanaka N, Desai D, Amin SG, Albert I, Patterson AD, Gonzalez FJ. Intestinal farnesoid X receptor signaling promotes nonalcoholic fatty liver disease. J Clin Invest. 2015; 125(1):386–402. [PubMed: 25500885]
15. Cummings JH. Short chain fatty acids in the human colon. Gut. 1981; 22(9):763–79. [PubMed: 7028579]
16. Hijova E, Chmelarova A. Short chain fatty acids and colonic health. Bratisl Lek Listy. 2007; 108(8):354–358. [PubMed: 18203540]
17. McNeil NI. The contribution of the large intestine to energy supplies in man. Am J Clin Nutr. 1984; 39(2):338–42. [PubMed: 6320630]
18. Zambell KL, Fitch MD, Fleming SE. Acetate and butyrate are the major substrates for de novo lipogenesis in rat colonic epithelial cells. J Nutr. 2003; 133(11):3509–3515. [PubMed: 14608066]
19. Zheng X, Qiu Y, Zhong W, Baxter S, Su M, Li Q, Xie G, Ore BM, Qiao S, Spencer MD, Zeisel SH, Zhou Z, Zhao A, Jia W. A targeted metabolomic protocol for short-chain fatty acids and branched-chain amino acids. Metabolomics. 2013; 9(4):818–827. [PubMed: 23997757]
20. Zhang L, Nichols RG, Correll J, Murray IA, Tanaka N, Smith PB, Hubbard TD, Sebastian A, Albert I, Hatzakis E, Gonzalez FJ, Perdew GH, Patterson AD. Persistent Organic Pollutants Modify Gut Microbiota-Host Metabolic Homeostasis in Mice Through Aryl Hydrocarbon Receptor Activation. Environ Health Perspect. 2015; 123(7):679–88. [PubMed: 25768209]
21. Schwiertz A, Taras D, Schafer K, Beijer S, Bos NA, Donus C, Hardt PD. Microbiota and SCFA in lean and overweight healthy subjects. Obesity. 2010; 18(1):190–5. [PubMed: 19498350]
22. Teixeira TF, Grzeskowiak L, Franceschini SC, Bressan J, Ferreira CL, Peluzio MC. Higher level of faecal SCFA in women correlates with metabolic syndrome risk factors. Br J Nutr. 2013; 109(5): 914–9. [PubMed: 23200109]
23. Pan YH, Zhang Y, Cui J, Liu Y, McAllan BM, Liao CC, Zhang S. Adaptation of phenylalanine and tyrosine catabolic pathway to hibernation in bats. PloS one. 2013; 8(4):e62039. [PubMed: 23620802]
24. Guinzberg R, Cortes D, Diaz-Cruz A, Riveros-Rosas H, Villalobos-Molina R, Pina E. Inosine released after hypoxia activates hepatic glucose liberation through A3 adenosine receptors. Am J Physiol Endocrinol Metab. 2006; 290(5):E940–51. [PubMed: 16352677]
25. Fernandes J, Su W, Rahat-Rozenbloom S, Wolever TMS, Comelli EM. Adiposity, gut microbiota and faecal short chain fatty acids are linked in adult humans. Nutr Diabetes. 2014; 4
26. Ley RE, Backhed F, Turnbaugh P, Lozupone CA, Knight RD, Gordon JI. Obesity alters gut microbial ecology. Proc Natl Acad Sci U S A. 2005; 102(31):11070–11075. [PubMed: 16033867]
27. Anderson JW, Bridges SR. Short-chain fatty acid fermentation products of plant fiber affect glucose metabolism of isolated rat hepatocytes. Proc Soc Exp Biol Med. 1984; 177(2):372–6. [PubMed: 6091151]
28. Reilly KJ, Rombeau JL. Metabolism and Potential Clinical-Applications of Short-Chain Fatty-Acids. Clin Nutr. 1993; 12:97–105.
29. Roy CC, Kien CL, Bouthillier L, Levy E. Short-chain fatty acids: ready for prime time? Nutr Clin Pract. 2006; 21(4):351–66. [PubMed: 16870803]
30. Aschenbach JR, Kristensen NB, Donkin SS, Hammon HM, Penner GB. Gluconeogenesis in Dairy Cows: The Secret of Making Sweet Milk from Sour Dough. IUBMB Life. 2010; 62(12):869–877. [PubMed: 21171012]
31. Banday AA, Marwaha A, Tallam LS, Lokhandwala MF. Tempol reduces oxidative stress, improves insulin sensitivity, decreases renal dopamine D1 receptor hyperphosphorylation, and restores D1 receptor-G-protein coupling and function in obese Zucker rats. Diabetes. 2005; 54(7):2219–26. [PubMed: 15983225]
32. Leighton F, Bergseth S, Rortveit T, Christiansen EN, Bremer J. Free Acetate Production by Rat Hepatocytes during Peroxisomal Fatty-Acid and Dicarboxylic-Acid Oxidation. J Biol Chem. 1989; 264(18):10347–10350. [PubMed: 2732225]
33. Hovik R, Brodal B, Bartlett K, Osmundsen H. Metabolism of Acetyl-Coa by Isolated Peroxisomal Fractions - Formation of Acetate and Acetoacetyl-Coa. J Lipid Res. 1991; 32(6):993–999. [PubMed: 1682408]

34. Mohamad-Shahi M, Karandish M, Haidari F, Omidian K, Fatemi-Tabatabayei SR, Rafiei H. Effect of daidzein-low-calorie diet on body weight, serum levels of glucose, resistin, and high sensitive C-reactive protein in high fat, high calorie diet induced rats. Saudi Med J. 2012; 33(1):70–5. [PubMed: 22273652]

35. Yamada KA. Calorie restriction and glucose regulation. Epilepsia. 2008; 49:94–96. [PubMed: 19049600]

36. Mehdad S, Hamrani A, El Kari K, El Hamdouchi A, Barakat A, El Mzibri M, Mokhtar N, Aguenaou H. Body mass index, waist circumference, body fat, fasting blood glucose in a sample of moroccan adolescents aged 11–17 years. J Nutr Metab. 2012; 2012:510458. [PubMed: 22175010]

37. Bakari AG, Onyemelukwe C, Sani BG, Aliyu S, Hassan SS, Aliyu TM. Relationship between casual blood sugar and body mass index in a suburban northern Nigerian population: a short communication. Niger J Me. 2007; 16(1):77–8.

38. Gladden LB. Lactate metabolism: a new paradigm for the third millennium. J Physiol. 2004; 558(Pt 1):5–30. [PubMed: 15131240]

39. DiGirolamo M, Newby FD, Lovejoy J. Lactate production in adipose tissue: a regulated function with extra-adipose implications. FASEB J. 1992; 6(7):2405–12. [PubMed: 1563593]

40. Beaufay H, De Duve C. The hexosephosphatase system. IV. Specificity of glucose-6-phosphatase. Bull Soc Chim Biol (Paris). 1954; 36(11–12):1525–37. [PubMed: 14378852]

41. Ren ZQ, Zhang PB, Zhang XZ, Chen SK, Zhang H, Lv DT, Zhuang BQ, Wen YQ, Hu HH, Ding WC, Zhang C. Duodenal-jejunal exclusion improves insulin resistance in type 2 diabetic rats by upregulating the hepatic insulin signaling pathway. Nutrition. 2015; 31(5):733–9. [PubMed: 25837221]

42. Ley RE, Turnbaugh PJ, Klein S, Gordon JI. Microbial ecology: human gut microbes associated with obesity. Nature. 2006; 444(7122):1022–3. [PubMed: 17183309]

43. Turnbaugh PJ, Backhed F, Fulton L, Gordon JI. Diet-induced obesity is linked to marked but reversible alterations in the mouse distal gut microbiome. Cell Host Microbe. 2008; 3(4):213–23. [PubMed: 18407065]

44. Furet JP, Kong LC, Tap J, Poitou C, Basdevant A, Bouillot JL, Mariat D, Corthier G, Dore J, Henegar C, Rizkalla S, Clement K. Differential adaptation of human gut microbiota to bariatric surgery-induced weight loss: links with metabolic and low-grade inflammation markers. Diabetes. 2010; 59(12):3049–57. [PubMed: 20876719]

45. Mitchell JB, Xavier S, DeLuca AM, Sowers AL, Cook JA, Krishna MC, Hahn SM, Russo A. A low molecular weight antioxidant decreases weight and lowers tumor incidence. Free Radic Biol Med. 2003; 34(1):93–102. [PubMed: 12498984]

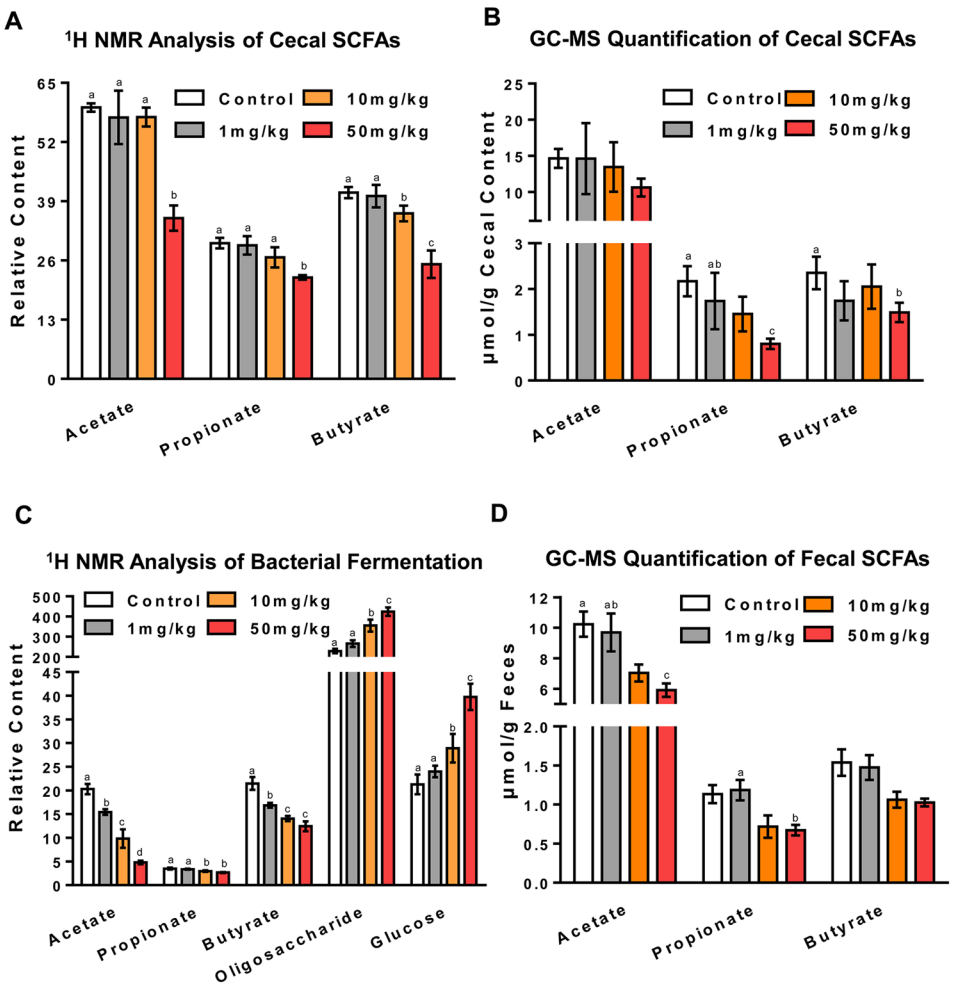

Figure 1.

Tempol inhibits gut microbiota fermentation in a dose-dependent manner. (A and C) Cecal content extracts and fecal metabolite changes were determined by ^{1}H NMR. Relative content of metabolites were determined by NMR peak integration compared to the internal standard TSP in the cecal content extracts and feces. Groups labeled with different letters are statistically significant ($p<0.05$), while groups sharing at least one letter are not significantly different. Groups without labels are not significantly different from other groups. (B and D) Quantification of SCFAs by GC-MS analysis was performed to validate results obtained via ^{1}H NMR. All data are presented as mean ± SEM. (n=5 mice per group) and analyzed using one-way ANOVA with Tukey's correction.

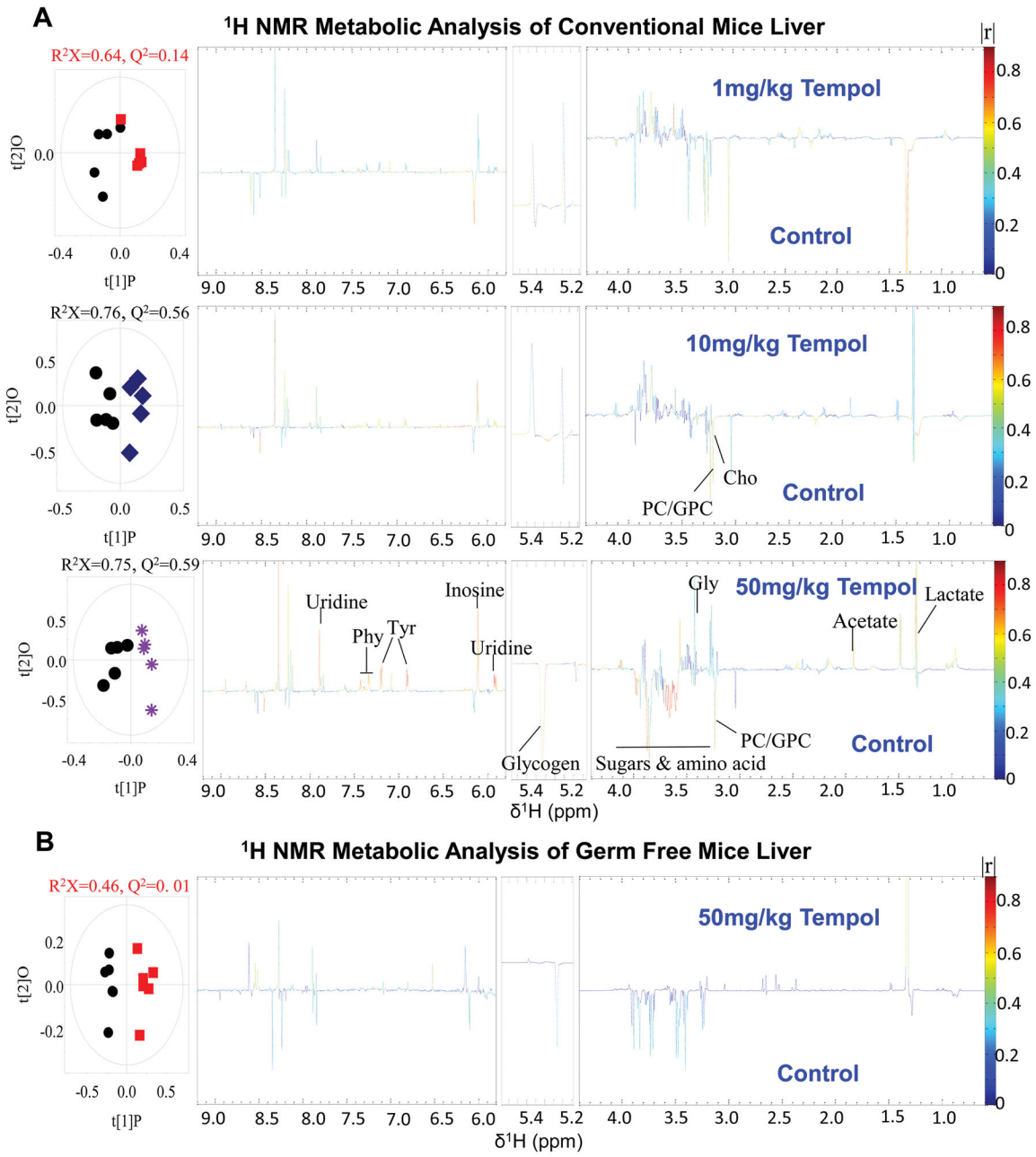

Figure 2.

Liver metabolism shifts to a more catabolic state in conventionally-raised mice treated with increasing doses of tempol. (A) Conventionally-raised mouse liver metabolic profiles of control group (black circles) and 1 mg/kg (red squares), 10 mg/kg (blue squares), and 50 mg/kg (purple asterisks) tempol groups determined by ^{1}H NMR. O-PLS-DA scores (left) and coefficient-coded loadings plots (right) for the models obtained from the ^{1}H NMR liver spectra (n=5 mice per group). (B) Comparison of germ-free mice liver metabolites between control group (back circles) and 50 mg/kg tempol group (red squares) determined by ^{1}H NMR (n=5 mice per group).

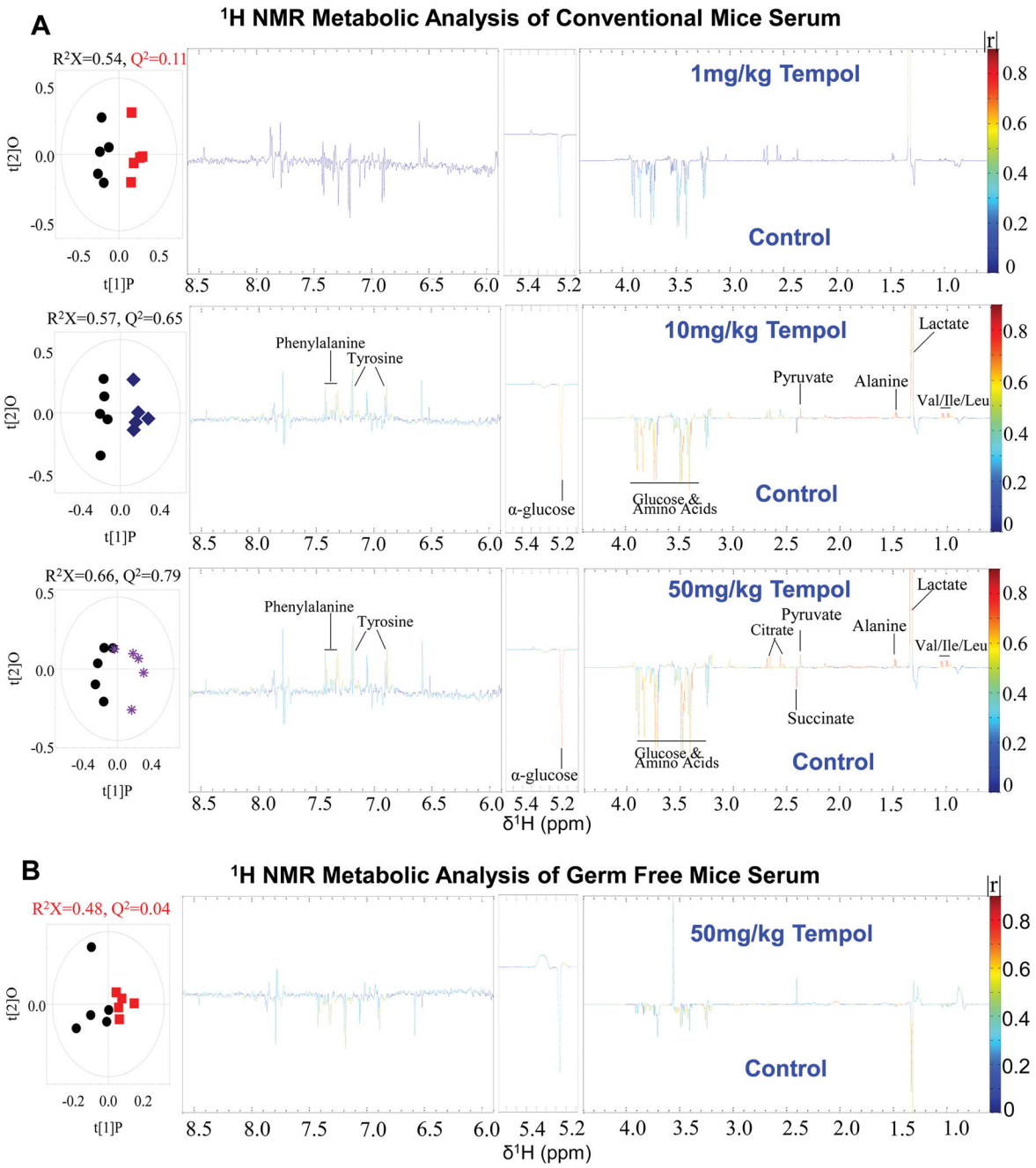

Figure 3.

Serum metabolites are associated with increased glycolysis in conventionally raised mice treated with increasing doses of tempol. (A) Comparison of serum metabolic profiles of conventionally-raised mice between control group (black circles) and 1 mg/kg (red squares), 10 mg/kg (blue squares), and 50 mg/kg (purple asterisks) tempol groups determined by ^{1}H NMR. O-PLS-DA scores (left) and the coefficient-coded loadings plots (right) for the models obtained from the NMR spectra of serum extracts (n=5 mice per group). (B)

Comparison of serum metabolites between control group (black circles) and 50 mg/kg tempol group (red squares) determined by ^{1}H NMR in germ-free mice (n=5 mice per group).

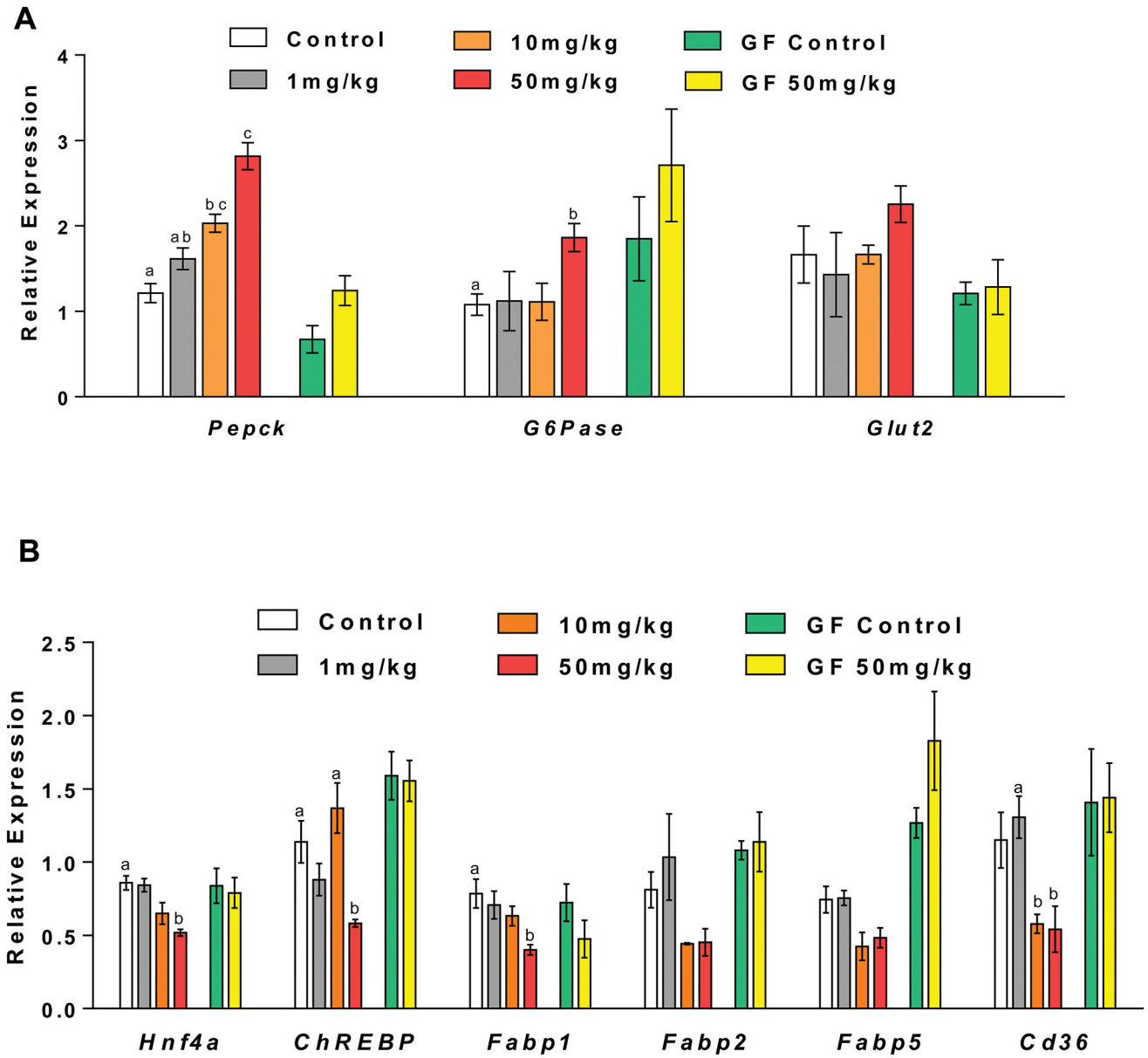

Figure 4.

Tempol altered hepatic expression of genes involved in glucose and lipid metabolism. QPCR analysis of hepatic mRNA levels of (A) glucose metabolism related genes, (B) lipid metabolism related genes in conventionally-raised and germ-free mice after 5-day tempol treatment. Groups with different letters are significantly different ($p<0.05$). Groups without labels are not significantly different from other groups. All data are presented as mean ± SEM (n=5 mice per group) and analyzed using one-way ANOVA with Tukey's correction, or two-tailed Student's t-test.